Environmental Pollution 267 (2020) 115683

Contents lists available at ScienceDirect

Environmental Pollution

journal homepage: www.elsevier.com/locate/envpol

Macro, colloidal and nanobiochar for oxytetracycline removal in synthetic hydrolyzed human urine☆

Sammani Ramanayaka [a], Manish Kumar [b], Thusitha Etampawala [c], Meththika Vithanage [a, *]

[a] Ecosphere Resilience Research Center, Faculty of Applied Sciences, University of Sri Jayewardenepura, Nugegoda, Sri Lanka
[b] Discipline of Earth Sciences, Indian Institute of Technology Gandhinagar, Gujarat, 382 355, India
[c] Department of Polymer Science, University of Sri Jayewardenepura, Nugegoda, Sri Lanka

ARTICLE INFO

Article history:
Received 30 May 2020
Received in revised form
8 August 2020
Accepted 15 September 2020
Available online 18 September 2020

Keywords:
Wastewater treatment
Engineered biochar
Pharmaceuticals
Adsorption
Water and sanitation

ABSTRACT

Macro (BC), colloidal (CBC) and nanobiochar (NBC) were examined for the particle size effect for adsorptive removal of oxytetracycline (OTC) and co-occurring nutrients, which are present in synthetic hydrolyzed human urine. The surface morphologies and functionality of biochars were characterized using Scanning Electron Microscopy (SEM), Brunauer-Emmett-Teller (BET) specific surface area and Fourier Transform Infra-Red (FTIR) Spectroscopy. Experiments for the removal of OTC were performed at the natural pH (pH 9.0) of hydrolyzed human urine using solid-solutions of 3 types of chars (1 g/L) with a contact time of 5 h, at initial OTC concentration of 50 mg/L where isotherm experiments were investigated with OTC concentrations from 25 to 1000 mg/L. The highest maximum adsorption capacity of 136.7 mg/g was reported for CBC, while BC reported slightly low value (129.34 mg/g). Interestingly, NBC demonstrated a two-step adsorption process with two adsorption capacities (16.9 and 113.2 mg/g). Colloidal biochar depicted the highest adsorption for NH_4^+, PO_4^{3-}, and SO_4^{2-} nutrients. All 3 types of chars showed strong retention with a poor desorption (6% in average) of OTC in synthetic hydrolyzed urine medium. CBC and NBC demonstrated both physisorption and chemisorption, whereas the OTC removal by BC was solely via physisorption. Nevertheless, CBC biochar demonstrated the best performance in adsorptive removal of OTC and nutrients in hydrolyzed human urine and its capability towards wastewater treatment. As the removal of nutrients were low, the treated urine can possibly be used as a safe fertilizer.

1. Introduction

Animal manure, sewage sludge and crop residues are some of the commonly used organic fertilizers, enriched with essential plant nutrients, which enhance crop productivity (Ahadi et al., 2020; Maillard and Angers, 2014; Nafi et al., 2020). Nevertheless, farmers tend to apply a few other types of organic fertilizers to fulfill the overall nutrient requirement. Among other organic fertilizers, human urine has been identified as an excellent mineral supplement (Pradhan et al., 2007). The composition of human urine along with the mixture of cations Na^+, K^+, NH_4^+, Ca^{2+} and anions, Cl^-, SO_4^{2-}, PO_4^{3-}, HCO_3^-, has the ability to improve crop production (Pandorf et al., 2018). Research studies have confirmed that NH_4^+ and phosphorous from PO_4^{3-} in urine have exhibited higher intake compared to other soluble phosphorous and NH_4^+ sources of organic fertilizers such as animal manure (Xu et al., 2018). However, in applying human urine to agricultural fields, some unavoidable circumstances may appear such as; contamination of heavy metals and pharmaceuticals (Sun et al., 2018). Concentrations of heavy metals were comparatively low in human urine, compared to other organic fertilizers (Medeiros et al., 2020). Nevertheless, Cu, Hg, Cd, Ni, and Zn concentrations were reported 10–500 times higher in urine than surface waters (Ogunfowokan et al., 2019). Besides that, the detection of pharmaceuticals in human urine has become the most significant concern in applying urine in farmlands (Arias et al., 2019; Pradhan et al., 2007). However, the application of human urine containing sludge from sewage and wastewater treatment plants is getting more popular than the direct application of urine in agricultural lands.

☆ This paper has been recommended for acceptance by Jörg Rinklebe.
* Corresponding author.
E-mail address: meththika@sjp.ac.lk (M. Vithanage).

https://doi.org/10.1016/j.envpol.2020.115683
0269-7491/

Human urine contains nearly two-thirds of active ingredients of consumed drug mass on average, which is health hazardous when released to the ecosystem (Bischel et al., 2015). Through surface runoff, these emerging contaminants can proliferate in soil and water bodies. Among many different types of pharmaceuticals, antibiotics are highly reported in urine and more than 75% excreted without undergo any metabolism (Katsikaros and Chrysikopoulos, 2020). Owing to the presence of antibiotics in natural environments, the development of antibiotic resistance in bacteria and endocrine-disrupting effects in aquatic life is a deleterious environmental impact (Sivagami et al., 2020). Oxytetracycline (OTC) is one of the most common broad spectrum antibiotics, which belongs to the tetracycline group and it has been used to treat a wide range of infectious diseases in both human and animal, as a growth promoter and a food additive for livestock (Harja and Ciobanu, 2018). As a broad-spectrum antibiotic, OTC act against both gram-positive and gram-negative bacteria (Ramanayaka et al., 2020a). Nevertheless, detection of OTC in the natural environment is comparatively high (5.0–5.7 μg/L) owing to the release of OTC via urine (Kaufmann et al., 2007). Detection of pharmaceuticals, especially antibiotics in wastewater, surface water and ground waters, leads to complex circumstances in the ecosystem. Antibiotics that have designed for specific physiological functions are possible to results in adverse effects on living beings (Ji et al., 2012). Research studies have confirmed that antibiotics in aqueous environments may tend to develop antibiotic resistance bacterial species, reproduction inhibition, or endocrine disruption (Ji et al., 2010; Park and Choi, 2008). Hence, the removal of these emerging contaminants before their environmental release is the need of the hour.

OTC is a large organic molecule that is undergo speciation. Between 3.5 and 7.5 pH, OTC demonstrates zwitterionic form, while below the 3.5 pH positively charged and above 7.5 pH, negatively charged (Premarathna et al., 2019). Conventional wastewater treatment plants are not capable of removing antibiotics. Literature confirms some other removal methodologies of pharmaceuticals from urine, such as ion exchange, advance oxidation, membrane separation and electrodialysis are highly selective and costly in operation (Solanki and Boyer, 2017). Despite, adsorption is often taken to be a preferable method to treat water due to the convenience, environmental friendliness, efficiency and applicability to the multi-component pollutant systems (Ramanayaka et al., 2020a; Tian et al., 2020). Consequently, it is essential to focus on adsorptive removal of antibiotics using a cost-efficient adsorbent material for removing pharmaceuticals from urine rich wastewaters due to the economic feasibility of the process, non-skilled secure handling, less toxicity, high performance, tunability, and environmentally friendly operation.

The adsorption capabilities of organic and inorganic compounds, including pharmaceuticals, have been studied with different adsorbent materials; clay, activated carbon and nanocomposites (Lin et al., 2005; Ramanayaka et al., 2020a; Yang et al., 2015). Among many adsorbents, research studies have confirmed biochar as an inexpensive, outstanding, eco-friendly adsorbent material/waste by-product (Foong et al., 2020; Kong et al., 2019). Feedstock type and high production temperature (>400 °C) directly influence the surface area and micropores of the material, which improves the adsorption capacity (Ahmad et al., 2014). Through surface modification methodologies, adsorption capacities of biochar can further be improved. Physical modification of biochar received recent attention as a greener and cost-effective technique than the chemical activation. Surface area and properties of biochar can be enhanced in advance by scaling down the size of biochar from the macro scale to nano scale, which is a physical modification (Ramanayaka et al., 2020b). Ball milling of macro biochar (BC) has been identified as the most popular method for the preparation of colloidal (CBC) and nanobiochar (NBC). Moreover, ball-milled biochar contains both nano and colloidal fractions that can be separated by following gravity separation techniques (Ramanayaka et al., 2020b). Colloidal biochar, which has a particle size of 100 nm–1 μm, is known as a by-product in the preparation of NBC (<100 nm). Literature suggests that colloidal biochar has a promising adsorption capacity compared to both macro and nanobiochar (Qian et al., 2016).

Despite the research reported high adsorptive removal of OTC using biochar, limited attempts have been adopted in place for its removal using colloidal and nanobiochar (Li et al., 2020; Ramanayaka et al., 2020b). At the same time, only a few research work had been reported on the adsorptive removal of pharmaceuticals from human urine (Solanki and Boyer, 2017). As the very first study, Solanki et al. (2017) have studied the removal of different types of pharmaceuticals i.e. pain relief, anti-inflammatory, an antidepressant with biochar and activated carbon for fresh and hydrolyzed urine and wastewater (Solanki and Boyer, 2017). The obtained results from batch tests exhibited that the biochars they have been used were able to remove more than 90% of pharmaceuticals while maintaining a co-removal of <20% for NH_4^+, and PO_4^{3-} found in urine and wastewater (Solanki and Boyer, 2017). Nevertheless, not many studies have focused on the removal of antibiotics in human urine using biochar (Sun et al., 2018). The limited research reports on the removal of antibiotics using colloidal and nanobiochar encourage us to carry out the removal of OTC from human urine with three different size fractions of biochars with following objectives; (i) to assess the adsorption capacities of macro, colloidal and nanobiochars for the removal of OTC in synthetic hydrolyzed human urine (ii) to understand the removal potential of co-occurring nutrients in urine and (iii) to postulate the adsorption mechanisms.

2. Materials and methods

2.1. Chemicals

Sodium chloride (NaCl; analytical reagent, 99%), sodium sulfate (Na_2SO_4; analytical grade, 99%), potassium chloride (KCl; analytical reagent, 99%), ammonium bicarbonate (NH_4CO_3; analytical reagent, 99%), monosodium phosphate ($NaH_2PO_4.2H_2O$; analytical reagent, 98%), disodium phosphate ($Na_2HPO4.7H_2O$; analytical reagent, 99.5%), ammonium hydroxide (NH_4OH; analytical reagent, 25%), Oxytetracycline (OTC; HPLC grade, 95%) were purchased from Sigma-Aldrich Co. Ltd. (United States). Deionized water was used in solution preparation.

2.2. Preparation of biochar

Dendro wood biochar *(Gliricidia sepium)*, which is a by-product of the gasification (700 °C), was collected from dendro thermal power plant, Thirappane, Sri Lanka. Collected sample of biochar was washed with distilled water, oven-dried at 60 °C and crushed into pieces using a mortar and pestle. Ground biochar was sieved using a mesh (<4 mm) and separated the macro fraction. Thereafter, sieved biochar was preconditioned at −80 °C for three days and ground for fine particles using a disk mill (Siebtechnik TS 250, Germany) (Ramanayaka et al., 2020b). Powdered biochar was suspended in ethanol and centrifuged at 1000 rpm for 2 min. The supernatant with nanofraction was collected, sonicated and dried on petri dishes using a vacuum oven at 50 °C. The dried layer of NBC is scraped off and collected (Ramanayaka et al., 2020b). The precipitated colloidal fraction in centrifugation was separately dried and collected for characterization and adsorption

experiments.

2.3. Preparation of synthetic hydrolyzed human urine

Human urine composition can be drastically varied depending on physiological factors, drug consumption and diet. Therefore, to maintain consistency and to avoid any disturbance for the experimental results due to drug contaminations, the synthetic composition of urine was utilized throughout the experiment series. Fresh urine is hydrolyzed in the aqueous environments; therefore, hydrolyzed urine has been used according to the objectives of the study. Hydrolyzed human urine was prepared based on the reported recipe in the literature (Solanki and Boyer, 2017; Zhang et al., 2015). We dissolved the required amounts of NaCl, Na_2SO_4, KCl, $NaH_2PO_4.2H_2O$, NH_4HCO_3, and NH_4OH in freshly prepared phosphate buffer solution at pH = 9 to prepare synthetic hydrolyzed human urine.

2.4. Characterization of biochars

Three types of biochars, macro, colloidal and nanobiochar, were characterized to investigate surface morphology, surface functional groups and specific surface area. Field-Emission Scanning Electron microscopy (FE-SEM; Hitachi SU6600, Japan) was used to inspect the surface topography of biochars. Different biochar samples were placed on a double-sided adhesive tape on the sample holder and subjected to gold sputtering before the samples were viewed under SEM. Surface functional groups of the materials were determined by Fourier Transform Infrared Spectroscopy (FTIR, Thermo Scientific Nicolet iS10, USA) in the wavelength range of 4000–550 cm^{-1}. The specific surface area of the chars was analyzed using Brunauer–Emmett–Teller (BET) surface area analyzer (Autosorb iQ Quantachrome Instruments, USA). Nitrogen adsorption isotherms of the three biochar samples at 77 K were obtained at the relative pressure range from 0.05 to 1. Prior to the analyses, the samples were outgassed at 300 °C for 3 h by applying a vacuum. Solution pH values were measured with a pH meter (Adwa AD1030, Romania). A nanoparticle analyzer (Horiba SZ-100, Japan) was used to analyze the size of NBC particles.

2.5. Kinetic experiments

Three adsorbents: macro, colloidal and nanobiochar were allowed to hydrate in synthetic hydrolyzed urine (300 mL) with a 1 g/L dosage for 5 min. Oxytetracycline (15 mg/L) was spiked separately into three different biochar suspended solutions. The suspensions were pipetted out at different time intervals from 10 to 240 min and filtered using a 0.45 μm syringe filter. Finally, filtered samples were analyzed at the wavelength of 356 nm using the UV–Vis spectrophotometer (Shimadzu UV160A, Japan).

2.6. Isotherm experiments

Isotherm experiments were carried out at ambient temperature (303 K) at a pH of 9, which is the pH of hydrolyzed urine. OTC concentrations from 25 to 1000 mg/L were maintained in the isotherm experiments with an adsorbent dosage of 1 g/L. After reaching equilibrium, samples were centrifuged and the supernatant was filtered with a 0.45 μm syringe filter. Finally, samples were analyzed. The adsorbed amount (q_e) of OTC (mg/g) was determined by using equation (1)

$$q_e = \frac{C_c - C_s}{C_m} \quad (1)$$

where q_e is the amount of OTC adsorbed onto BC, CBC, NBC; C_s is the adsorbate concentration (mg/L) in the supernatant of the sample; C_c is the adsorbate concentration (mg/L) in control; and C_m is the BC, CBC, and NBC concentration (g/L).

2.7. Desorption experiments

A 50 mg/L OTC was spiked to BC, CBC, and NBC solutions (1 g/L) and allowed to adsorb for 5 h. From each, 100 mL of the slurry solution was withdrawn and washed with deionized water for 3 times. Then synthetic hydrolyzed urine was added to samples and kept for desorption in a shaker for 15 min. Finally, samples were filtered and the filtrate was analyzed in UV–Vis spectrophotometer.

2.8. Nutrient analysis

Adsorption of nutrients for each type of char was analyzed for pure urine and in 3 time intervals during OTC adsorption (50 mg/g). Samples (5 mL) were pipetted out and filtered. The filtrate was analyzed for NH_4^+, PO_4^{3-}, and SO_4^{2-} with time intervals of 2, 40 and 300 min using DR 900, USA portable colorimeter. Ammonia Nitrogen Test Kit with salicylate and cyanurate powder pillows were used to analyze NH_4^+. For 10 mL of sample, ammonium salicylate was added and kept for 3 min and then cyanurate was added. Before analysis solution was kept for a 15 min for the reaction to take place. Acid persulfate digestion method was used to analyze PO_4^{3-} while SulfaVer 4 Reagent Powder was used in the analysis of SO_4^{2-}. Each powder pillow was kept for 2 min and 5 min intervals respectively to undergo reaction before the analysis (Wijesekara et al., 2014).

2.9. Data analysis

Isotherm data was modeled using Origin 8 Pro software with Hills, Langmuir and Freundlich models to evaluate the best-fit curve, maximum adsorption capacity and equilibrium time. The isotherm model, which yields the best-fit curve, has been selected with the correlation coefficient (R^2), which is the closest to +1. FTIR data were analyzed were conducted using OMINIC Version 9.9 0.473 software.

3. Results and discussion

3.1. Characterization of biochar

The variation of surface morphologies is essential to understand surface heterogeneity and to support bet surface area (BET) analysis. Furthermore, the number of available functional groups, as well as the type of groups, directly influence the maximum adsorption capacities of the material. The available functional groups were identified for the three types of biochars. The yield of nanobiochar is considerably low compared to the yield of colloidal biochar.

3.1.1. Scanning electron microscopic analysis (SEM)

The SEM images of BC, CBC and NBC under three different magnifications (x900, x60 and x70K) are shown in Fig. 1. Microscopic topologies and extremely porous structure of BC can be clearly seen in the image (a). Randomly distributed macro and meso pores have been observed in SEM images and these large pores may influence immobilization of OTC via pore filling

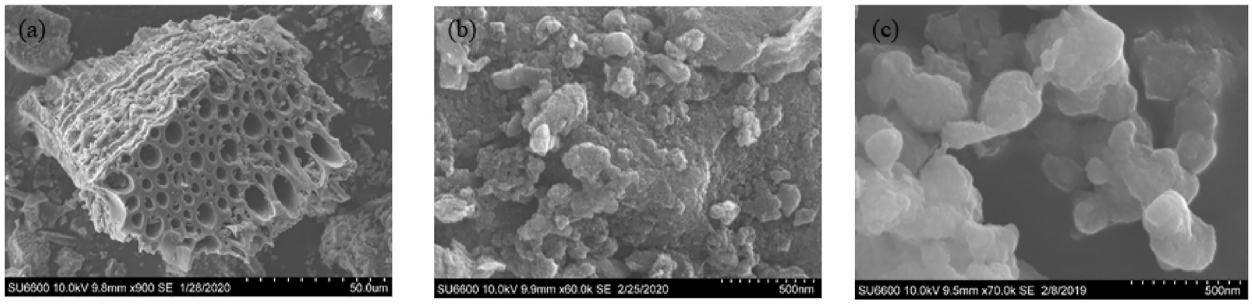

Fig. 1. SEM images of (a) BC, (b) CBC and (c) NBC. Both CBC and NBC demonstrate occasional aggregates.

mechanism. CBC and NBC are more like to be agglomerated owing to static charges between particles (Ramanayaka et al., 2020b). The SEM images of CBC and NBC demonstrated destruction of pores due to mechanical grinding. Graphitic nature and aggregation of NBC was clearly visible in SEM images. This aggregation may create solute transport channels which will help trapping OTC to biochar flakes in weak bonds.

3.1.2. Fourier transform infrared analysis (FTIR)

Pristine BC, CBC and NBC demonstrate three different FTIR patterns, confirming surface functional groups are influenced by the downscaling of biochar (Fig. 2). The strong, broad peak at 3420 cm^{-1} exhibited phenolic −OH stretching in all three types of biochar while, CBC determined a medium peak at 3126 cm^{-1} which is possibly a C=C stretching (Ramanayaka et al., 2020b). The alkane groups have manifested by peaks at 2924 and 2852 cm^{-1} which is clearly visible only on BC (Herath et al., 2015). The emergence of aromatic C=C stretch around 1654 cm^{-1} in NBC FTIR spectrum may be due to structural differences that can occur with respect to the milling process (Qian et al., 2016). Both BC and CBC exhibited C=C peaks around 1569 cm^{-1}. Moreover, in BC FTIR spectrum, C−H bending peak around 1430 cm^{-1}, has been shifted to lower wavenumber, 1390 cm^{-1} in CBC and 1385 cm^{-1} in NBC respectively, which is known as a red shift. The alcoholic bond C−O (1083 cm^{-1}), again demonstrated a red shift from BC to NBC, which confirms the effect of ethanol, used in the milling process (Bandara et al., 2017).

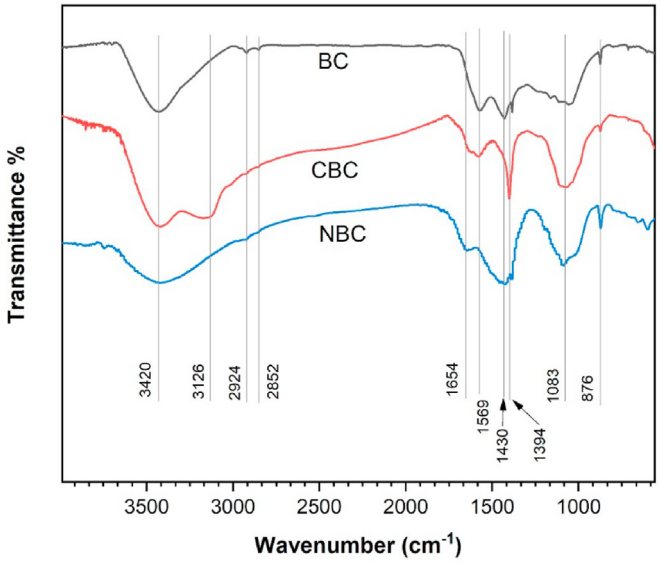

Fig. 2. FTIR spectrums of pristine macro, colloidal and nanobiochar.

Furthermore, the peak around 876 cm^{-1}, exhibited aromatic C=CH bond in all three types of biochar (Mayakaduwa et al., 2016).

3.1.3. Bet surface area analysis (BET)

The analysis of BET specific surface area confirms that BC has a slightly higher specific surface area, specific total pore volume and average pore diameter than CBC (Table 1). However, the milling process of BC into NBC may reduce the specific surface area by approximately one order of magnitude, the total pore volume and average pore diameter by three folds. Consequently, the specific surface area of CBC is slightly higher than that of BC. Interestingly, the milling process of biochar broke down porous structures into small flakes having almost no pores. Furthermore, the smaller particles produced during the milling process can partially fill and block the existing pores in NBC samples. Thus, comparatively different sets of surface characteristics were observed on NBC. The material is porous or, in other words porosity of the biochar, samples were varied as CBC > BC > NBC according to the BET analysis.

Similar to the surface characteristics, N_2 adsorption isotherms of BC and CBC are almost similar and NBC is different from BC and CBC, as shown in Fig. 3a–c. For both BC and CBC the Type II isotherm was observed, while NBC as defined as a Type III isotherm by the IUPAC. In general, Type II isotherms are observed for mono- and multilayer adsorption of adsorbent molecules, while Type III isotherms are observed for the sheet-like structures as of graphite where the adsorbate − adsorbent interactions are relatively weak. Thus, the gas-adsorption isotherms further confirmed the graphitic structure of the NBC. The N_2 adsorption isotherms of all the biochar samples do not flatten at the highest relative pressure that was measured. This is attributed to the non-rigid aggregation of the biochar particles.

3.2. Biochar − oxytetracycline interaction studies

3.2.1. Kinetic effect on adsorption

The effect of reaction time for OTC adsorption on to BC, CBC, and NBC in a duration of 5 h was studied until the adsorption reached equilibrium and demonstrated in Fig. 4. BC has exhibited a gradually increasing adsorption of OTC for more than 2 h and was able to remove around 25% of OTC within 5 h (Fig. 4a). The elovich and pseudo-second-order models were fitted, however, the elovich model was revealed as the best fit according to the correlation coefficient (R^2) of 0.965 (Table 2). The pseudo second order model was only able to achieve a R^2 of 0.924. Nevertheless, both models were revealed the ion-exchange between surface chemisorption process, which is a specific adsorption (Ashiq et al., 2019; Wu et al., 2009). The macro pores present in BC may influence the adsorption of approximately 25% of OTC within 5 h. Furthermore, CBC, which has almost similar surface area to BC, demonstrated elovich model as the best fit model with a R^2 of 0.975. However, around 50% of

Table 1
Specific surface area, total pore volume and average pore diameter of biochar samples processed at different conditions.

Sample[a]	Specific surface area (m^2/g)	Specific total pore volume (cm^3/g)	Average pore diameter (nm)
BC	260.83	0.1731	2.654
CBC	284.28	0.1947	2.740
NBC	28.56	0.0635	0.891

[a] The R^2 of the best fits of the data to BET equation are 0.998, 0.998 and 0.997 for BC, CBC and NBC, respectively.

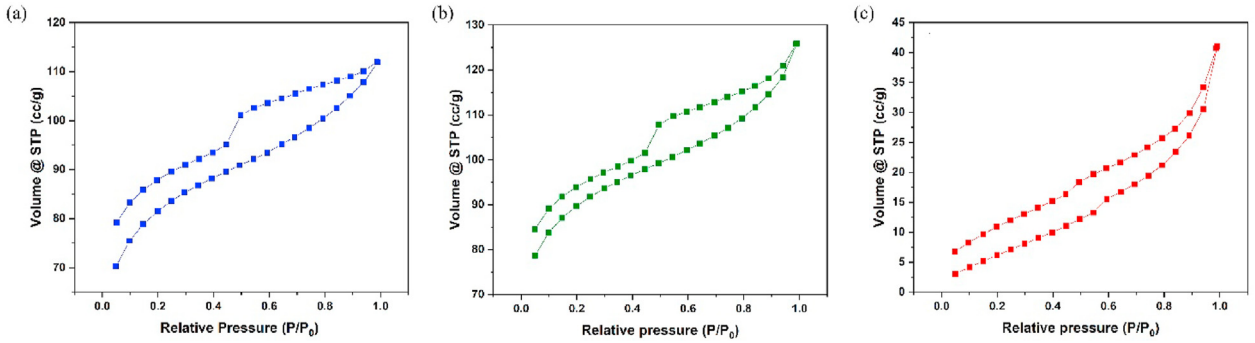

Fig. 3. Nitrogen adsorption and desorption isotherms of (a) BC, (b) CBC, and (c) NBC biochars.

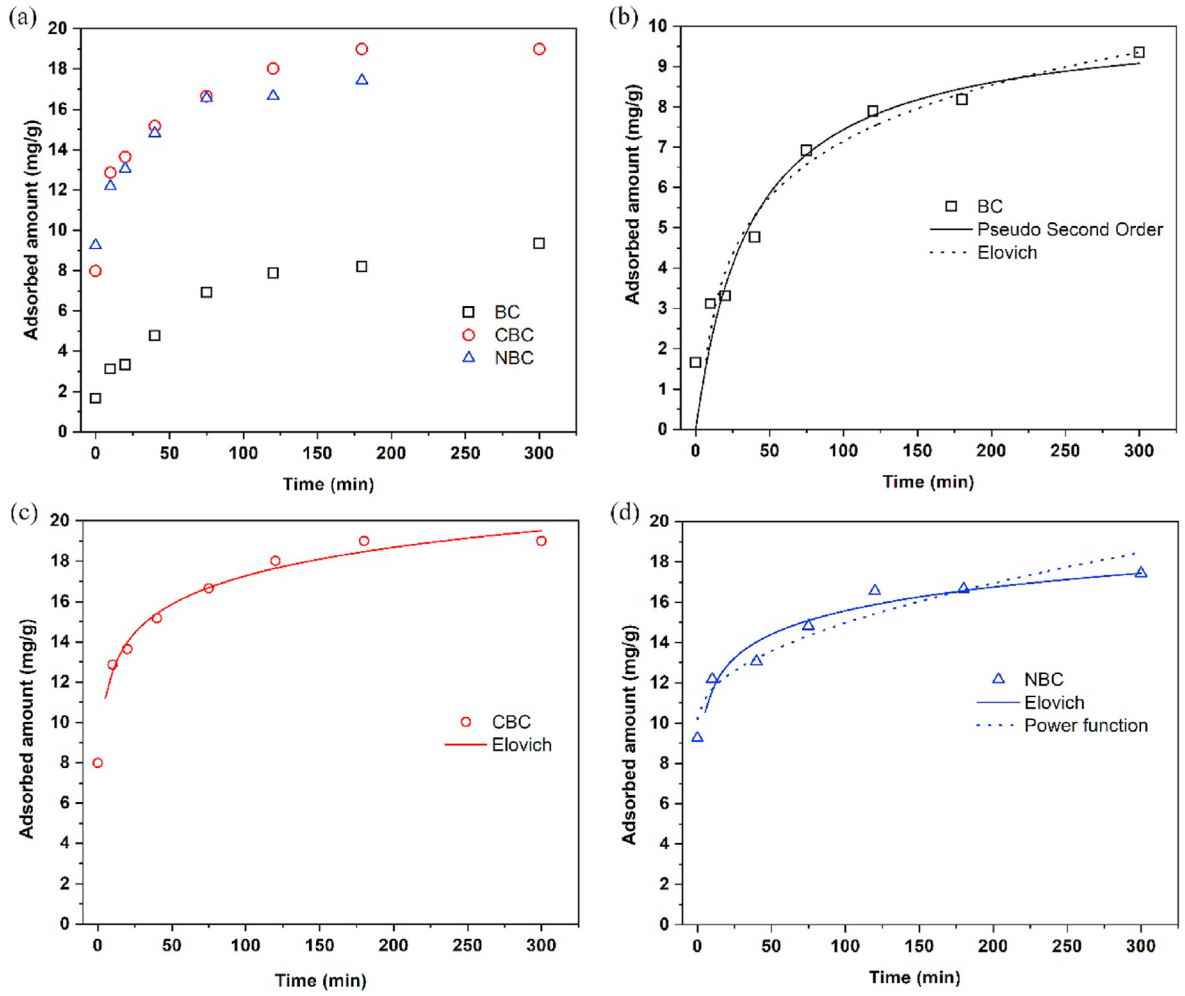

Fig. 4. (a) Effect of time on OTC adsorption by BC, CBC, and NBC at 1 g/L adsorbent dosage, at pH 9 with 50 mg/L OTC. Kinetic data of (b) BC, (c) CBC and (d) NBC fits for Pseudo second order and Elovich and power function equations.

Table 2
Isotherm and kinetic model parameters for the adsorption of OTC, on BC, CBC, and NBC at 1 g/L loading.

Experimentation	Model	Parameters	Value
Isotherm for BC	Freundlich $q_e = k_f C_e^n$	K_f (mg/g)/(mg/L)^n	2.806
		n	0.56
		R^2	0.994
		Chi^2	2.921
Isotherm for CBC	Hills $q_{ads} = \frac{q_{s_H} C_e^{n_H}}{K_D + C_e^{n_H}}$	K_D	0.004
		n_H	1.092
		Q_{max} (mg/g)	123.87
		R^2	0.972
		Chi^2	38.60
	Langmuir $R_L = \frac{1}{1 + K_L C_o}$	Q_{max} (mg/g)	136.7
		K (L/mg)	0.003
		R^2	0.972
		Chi^2	29.1
Isotherm for NBC	Langmuir	Q_{max} (mg/g)	16.87
		K (L/mg)	0.077
		R^2	0.923
		Chi^2	1.078
	Hills	K_D	0.004
		n_H	1.941
		Q_{max} (mg/g)	113.205
		R^2	0.965
		Chi^2	50.568
Kinetic for BC	Pseudo second order $\frac{d_{q_t}}{dt} = k_2(q_e - q_t)^2$	k_2 [g/(mg min)]	0.003
		q_e (mg/g)	10.206
		R^2	0.925
		Chi^2	0.692
	Elovich $\frac{d_{q_t}}{dt} = \alpha \exp(-\beta q t)$	α_E [mg/(g min)]	0.708
		β_E (g/mg)	0.498
		R^2	0.965
		Chi^2	0.257
Kinetics for CBC	Elovich	α_E [mg/(g min)]	98.6
		β_E (g/mg)	0.491
		R^2	0.975
		Chi^2	0.189
Kinetics for NBC	Elovich	α_E [mg/(g min)]	167.735
		β_E (g/mg)	0.591
		R^2	0.924
		Chi^2	0.434
	Power function	a	10.199
		kp	0.477
		R^2	0.929
		Chi^2	0.742

OTC was adsorbed within 5 h, revealing the excellent adsorption capacity of CBC over BC (Fig. 4b). The generation of new functional groups during the preparation process of CBC may attribute the considerable gap of OTC removal that is observed. Similar to BC, CBC also demonstrated a chemisorption process in the adsorptive removal of OTC (Wu et al., 2009). Moreover, fast adsorption of OTC has exhibited by NBC (Fig. 4c). Within the first hour, NBC has been adsorbed around 15 mg/g of adsorbate out of the solution. In 5 h, approximately 45% of OTC has been adsorbed. However, BC and CBC with macro and mesopores demonstrated elevated surface areas. NBC itself has a limited amount of pores and the remaining pores also possible to block with ultra-small nanoparticles. Therefore, the results obtained confirm that the surface area of a material depends on the pores which are present in the material. NBC depicted both elovich and power function models as the best-fitted models and at the same time with more similar R^2 values of 0.923 and 0.929 respectively. Power function has been modified from freundlich isotherm equation, which endorses physical adsorption process (Segun Esan et al., 2014). Interestingly, kinetic data modeling for NBC confirms a chemisorption process and a physisorption process, where both specific and non-specific adsorption have been carried out in the same period of time.

3.2.2. Adsorption isotherm experiments

The adsorbed amounts of OTC vs. the equilibrium concentrations of BC, CBC, and NBC is manifested in Fig. 3. All three types of biochar have not reached equilibrium within the experimental concentration range used in this series of experiments. Moreover, NBC was demonstrated a diverse behavior, which is a two-step equilibrium process. It has reached equilibrium in the first five data points and again demonstrated increasing adsorption until it reaches equilibrium. The maximum adsorption capacity (Q_{max}) for macrobiochar (BC) was reported at 129.34 mg/g, whereas, for colloidal biochar (CBC) at 136.7 mg/g. However, nanobiochar (NBC) demonstrated two maximum adsorption capacities, which is 16.9 mg/g, firstly and then again 113.2 mg/g. The best-fitted models for BC and CBC were Freundlich ($R^2 = 0.994$) and Hills ($R^2 = 0.972$) models, respectively. Nevertheless, Langmuir ($R^2 = 0.923$) and Hills ($R^2 = 0.965$) models were the best fit for NBC (Table 2).

Freundlich model demonstrated a heterogeneous substrate, which has an exponential distribution of energies and active sites. The foremost binding sites energies were comparatively high and exhibited an exponential decrease with the completion of the outermost layers (Garcıa et al., 2004). Therefore, multilayer adsorption has been hypothesized by the Freundlich model, which is a physisorption process (Ayawei et al., 2017). The adsorption strength of the contaminant on to adsorbent or the heterogeneity of the surface is indicated by 'n' in the Freundlich equation. Favorable adsorption of the contaminant has designated with the value of $n > 1$ and lower or values which are closer to zero demonstrate increasing heterogeneity, with increasingly nonlinear isotherm (Rao et al., 2009). Therefore, the isotherm of BC revealed favorable adsorption by denoting $n = 0.5$, which is lower than 1 (Fig. 5a).

Binding of different species onto a homogeneous adsorbent surfaces is the hypothesis behind Hills isotherm model. A cooperative phenomenon is observed through the binding of adsorbate molecules onto a single binding site influencing the other sites (Farouq and Yousef, 2015). Hills model discloses three different possibilities of binding ligands onto substrates: (1) positive cooperative binding $n_H > 1$, (2) non-cooperative or hyperbolic binding $n_H = 1$, and (3) negative cooperative binding of $n_H < 1$ (Saadi et al., 2015). Nevertheless, CBC demonstrated a positive, cooperative binding with n_H of 0.004. Similarly, the second step of NBC isotherm successfully fitted for Hills model and was exhibited positive, cooperative adsorption with n_H of 0.003. Consequently, Hills model exhibited physisorption, which is a non-specific adsorption.

Langmuir isotherm is the simplest model and assumes monolayer adsorption of ligands (Saadi et al., 2015). A single layer of molecules binds with uniform adsorption energy, onto the homogeneous adsorption surface of the adsorbent. Further adsorption is impossible once the adsorbate occupies a binding site (Ayawei et al., 2017). The first step of the NBC isotherm curve reveals monolayer adsorption behavior with specific adsorption, which is a chemisorption process (Fig. 5c). However, both Hills and Langmuir models were successfully fitted with CBC isotherm curve, almost overlap one another (Fig. 5b). Therefore, CBC demonstrates both chemisorption and physisorption in the adsorption process.

3.2.2.1. Partition coefficient. The adsorption capacity determines the removal potential of adsorbate from aqueous media. Nevertheless, a comparison of maximum adsorption capacities is unsuccessful owing to different initial concentrations used in experiments. Therefore, by considering only a high adsorption capacity, it is not possible to conclude the adsorption capacity. To overcome this concern, the partition coefficient (PC) value is introduced. PC represents the ratio between the sorbed adsorbate and the equilibrium concentration of adsorbate (Vikrant and Kim,

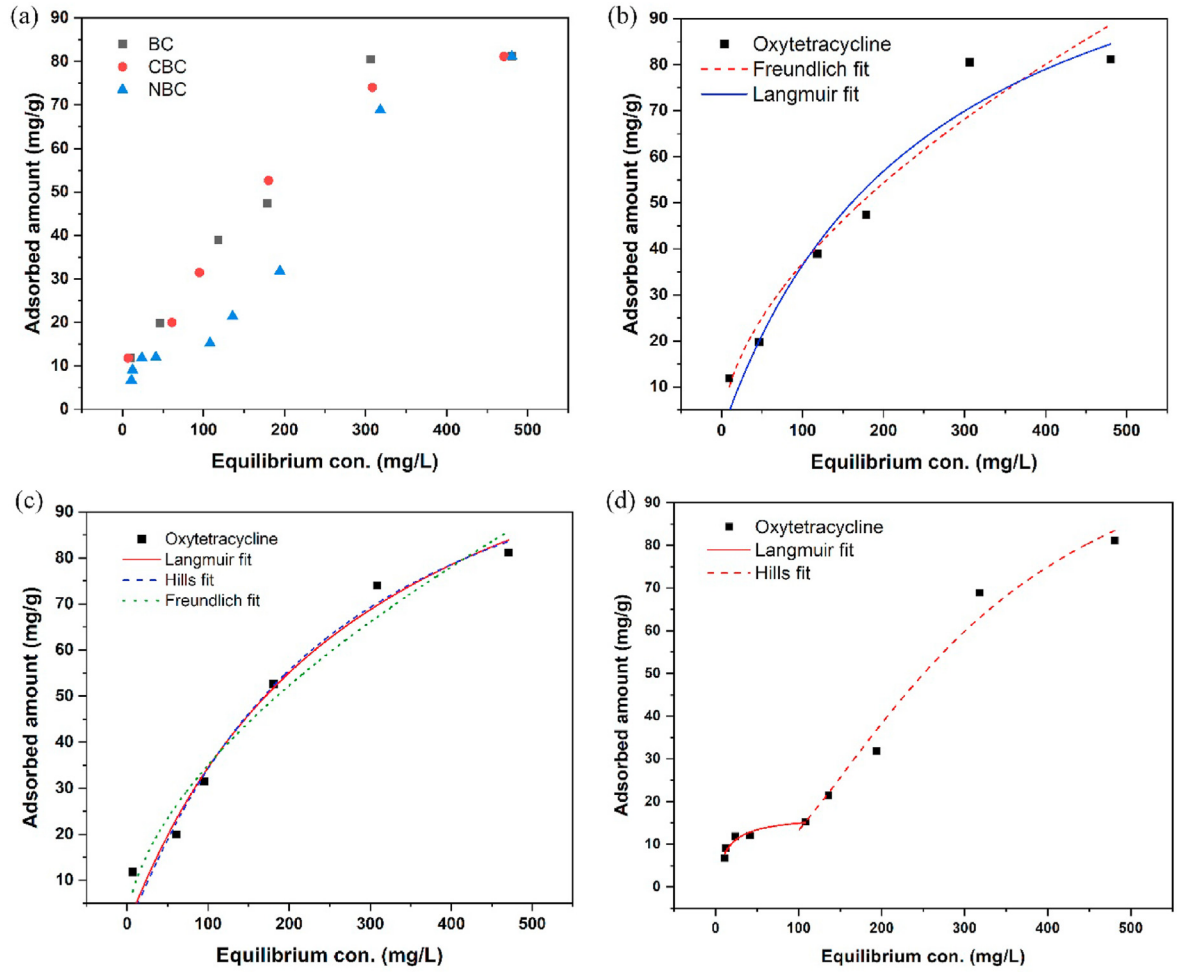

Fig. 5. Experimental data of initial OTC concentrations vs. adsorbed amounts (a) at pH 9, (b) BC, (c) CBC, and (d) NBC dosage of 1 g/L. Symbols represent experimental data, whereas lines indicate modeled data using the nonlinear least-squares fit of Hills, Langmuir and Freundlich equations.

2019). Performances of adsorbents can be compared with each other by using PC values without any distraction of initial concentrations etc. Dividing maximum adsorption capacity (mg/g) of sorbent by equilibrium concentration (mg/L) results in the PC of an adsorbent (Vikrant and Kim, 2019).

Table 3 demonstrates the PC values and a comparison of different biochars in antibiotic removal. In this study, we have reported high maximum adsorption capacities, nevertheless comparatively low PC values for macro, colloidal and nanoscale dendrobiochar. Many studies have assessed OTC removal utilizing biochar as the medium in aqueous media demonstrating low-average removal capacities i.e. Maize straw, pineapple peel (1.56 mg/g), and Cassava waste (3.33 mg/g) (Fu et al., 2016; Jia et al., 2013; Luo et al., 2018). Biochar has then been modified using chemical activation methods to improve its OTC remediation potential (Aghababaei et al., 2017; Feng et al., 2020; Wang et al., 2019). An interesting modification showed an enormously higher adsorption capacity of 360.5 mg/g compared to pristine and modified biochars by MnO_2 loaded bamboo willow biochar (20:1) (Feng et al., 2020). However, only a single study reported the possibility of biochar in removing OTC in hydrolyzed urine. Sun et al. (2018) have recounted comparatively high PC values in the adsorption of sulfonamide antibiotics onto cotton stalk biochar (Sun et al., 2018). Similar PC values reported for BC, CBC, and NBC (0.17 L/g) confirmed that the effects of particles size dose not influence the adsorption performance of dendrobiochar. The difference between PC values of cotton stalk biochar may be due to the differences in: (1) Chemical structures of two different classes of antibiotics, (2) Speciation, (3) The types of feedstock that has be used to prepare biochar and (4) Pyrolysis temperatures of biochar.

3.2.3. Desorption of OTC

Suspensions of OTC (50 mg/L) loaded BC, CBC and, NBC (1 g/L) were demonstrated extremely low desorption concentrations. Initially, 50 mg/L of OTC was introduced to the solution and after 12 h of adsorption time, only 30 mg/L of OTC was remaining in both CBC and NBC solutions. However, in the case of BC about 40 mg/L of OTC was adsorbed. Interestingly, 2.7 mg/L of OTC has been desorbed to urine from BC while, CBC and NBC have exhibited slightly higher desorption amounts; 3.0 and 3.2 mg/L, respectively. Desorption capacities of three different biochars corroborate with the findings of isotherms. OTC adsorption to BC indicated to be chemisorptive type, whereas CBC and NBC demonstrated more hybrid adsorption nature with physisorption followed by chemisorption. Hence, CBC and NBC were exhibited similar desorption capacities, 9.6 and 9.8%, respectively. As physisorption was higher in the case of NBC than that of the other two biochars, it showed slightly higher desorption as well. Nevertheless, BC exhibited

Table 3
Performance of removing contaminants from aqueous and urine media using pristine and modified biochars.

Material type	Feedstock material	Experimental medium	Contaminant	Maximum adsorption capacity (mg/g)	Adsorbent dosage (mg/L)	PC value L/g	Temperature °C	pH	Reference
Pristine biochar	Maize straw	Aqueous media	Oxytetracycline	-	5	0.04	298	5.5	Jia et al., 2013
Cassava waste biochar	Cassava waste	Aqueous media	Oxytetracycline	3.33	10	-	298	-	Luo et al., 2018
KOH-modified cassava waste biochar				10	10	-	298	-	
Magnetic attapulgite–biochar composite	Cauliflower leaves	Aqueous media	Oxytetracycline	33.31	2	-	298	-	Wang et al., 2019
MnO_2 loaded bamboo willow biochar (20:1)	Bamboo willow	Aqueous media	Oxytetracycline	360.5	0.66	–	298	5	Feng et al., 2020
Chemically activated forest residue biochar	5M H_3PO_4 forest residue	Aqueous media	Oxytetracycline	263.8	0.5	4.79	313	4	Aghababaei et al., 2017
Chemically activated wood-processing residue biochar	5M H_3PO_4 wood-processing residue			254.1	0.5	4.44	313		
Pineapple peel waste biochar	Pineapple peel	Aqueous media	Oxytetracycline	1.56	10	0.24	308	-	Fu et al., 2016
Cotton stalks biochar	Cotton stalks	Synthetic hydrolyzed urine	Sulfamethoxazole	0.003	1	0.53	298	9	Sun et al., 2018
			Sulfadiazine	0.001	1	0.54	298		
			Sulfadimethoxine	0.004	1	0.98	298		
			Sulfamethazine	0.003	1	0.94	298		
Dendro wood macro biochar (BC)	Dendro wood	Synthetic hydrolyzed urine	Oxytetracycline	129.34	1	0.17	298	9	This study
Dendro wood colloidal biochar (CBC)				136.7	1	0.17	298		
Dendro wood nano biochar (NBC)				113.2	1	0.17	298		

comparatively low desorption (6.75% of adsorbed amount). In the case of desorption, BC demonstrates better performance over both CBC and NBC.

3.2.4. Nutrient adsorption

In the presence of OTC (50 mg/L) adsorbed amounts of NH_4^+, PO_4^{3-}, and SO_4^{2-} onto BC, CBC, and NBC in 2, 40 and 300 min time intervals are shown in Fig. 6. Pure synthetic hydrolyzed urine depicted 5.3, 13.4, and 0.8 g/L of total adsorbed NH_4^+, PO_4^{3-}, and SO_4^{2-} amounts, respectively. After 2 min from introducing chars to the solution, PO_4^{3-} is the highest adsorbed nutrient by BC (2 g/L) which demonstrates a rapid adsorption. However, there was not any significant differences in the adsorption of PO_4^{3-} onto BC, CBC, and NBC, and SO_4^{2-} was exhibited the least adsorption within the first 2 min. PO_4^{3-} adsorption for 5 h is almost the same for 3 types of chars (2–2.3 g/L). However, NBC reaches a little high adsorption of 2.5 g/L after 5 h. A gradual increment of SO_4^{2-} adsorption to BC, CBC, and NBC has been observed with increasing time. Nevertheless, all 3 types of biochars have exhibited similar adsorption capabilities of NH_4^+ adsorption after 5 h (1.1–1.2 g/L). The negatively charged PO_4^{3-}, and SO_4^{2-} nutrients demonstrated an approximately 18% adsorption after 5 h, while NH_4^+ showed 22% with a slight increase. The difference between the adsorption percentages of two nutrient types may be due to the repellence of negatively charged nutrients by the negatively charged biochar surface. Therefore, NH_4^+ has favor in the adsorption process, which is visible from the increase in adsorption percentage. However, the results confirm that there is a competition between OTC molecules and nutrients in surface adsorption.

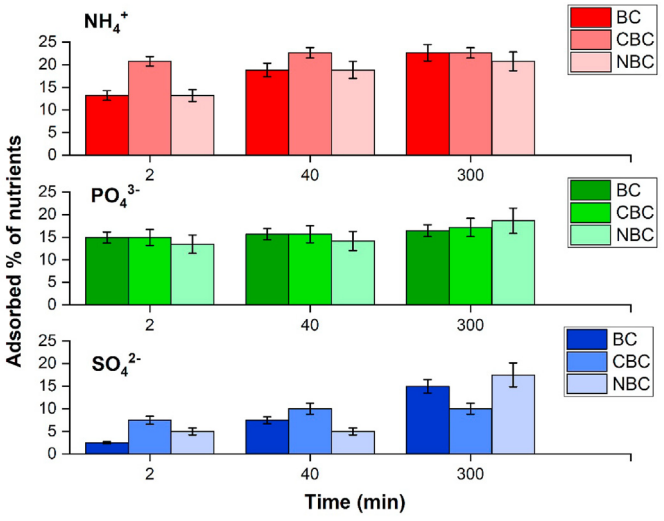

Fig. 6. Nutrients (NH_4^+, PO_4^{3-}, and SO_4^{2-}) adsorption capacities onto BC, CBC, and NBC (1 g/L) for 5 h with a 50 mg/L of OTC.

3.2.5. Influence of surface functional groups

The peak analysis of FTIR spectrums, after the adsorption process, elucidate the peak shifts, increased intensities, disappearance and appearance of peaks (Fig. 7a–c). OTC loaded biochar FTIR spectrums have been compared with the spectrums of the same material before adsorption. Hydrolyzed human urine contains a considerably high amount of –OH and N–H groups. Broad peak around 3450 cm^{-1} and medium peak at 3150 cm^{-1} confirms the presence of –OH and C–H groups in both pristine biochar in urine and OTC loaded biochar for all three sizes. The effect of C–H bonds in OTC also can influence the peak around 3150 cm^{-1} and a new C–H alkane stretch has appeared around 2920 cm^{-1} in contaminant loaded adsorbents: BC, CBC and NBC, maybe due to the new bond formation with OTC adsorption (Nanda et al., 2013). Both BC and NBC have revealed a decrease in the stretching of C=O group of amides ($-CONH_2$) around 1620-1680 cm^{-1} with the adsorption of OTC; however, in CBC opposite phenomenon was observed (Ramanayaka et al., 2020b). All three types of pristine biochars manifested a sharp –COO bending peak around 1400 cm^{-1} and a decrease can be observed after adsorption (Tong et al., 2011). A sharp peak, which exhibited silicate structure and alcoholic C–O is showed in the range of 1050 with a decreasing intensity after contaminant loading. At pH 9, ionizable functional groups of OTC, are deprotonated to form anionic species of the molecule (Kong et al., 2012). Cations such as NH_4^+ are favorable in the formation of a positively charged layer with biochar surface functional groups

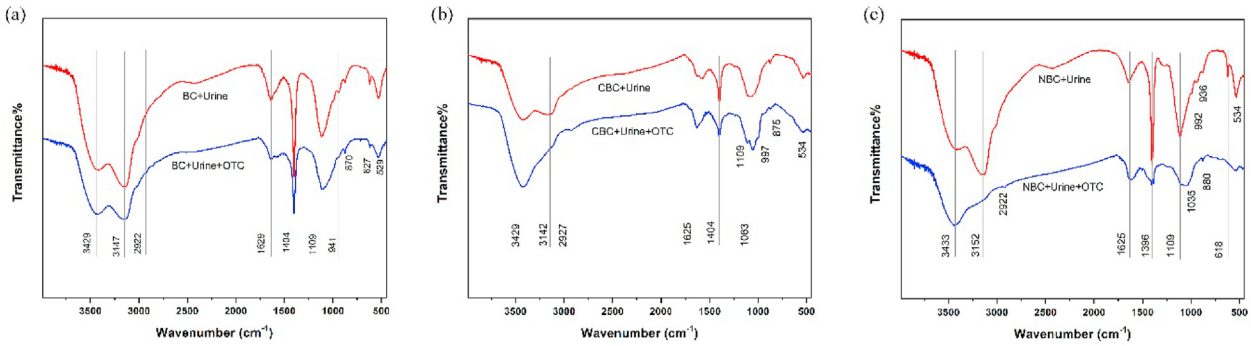

Fig. 7. Comparison of FTIR patterns for (a) BC, (b) CBC and (c) NBC biochars with urine and after adsorption of OTC.

such as amide ($-CONH_2$), alcoholic C—O and —COO, resulting in a multilayer formation. Negatively charged OTC molecules demonstrate a high affinity towards the positive layer and bind through the physisorption mechanism. Nevertheless, CBC and NBC have demonstrated a shoulder around 1063 and 1035 $cm^{-1,}$ which may be due to the addition of ethanol in the milling process (Manna et al., 2020). The high carbon content of biochar is undoubtedly seen in alkene and alkane peaks of the FTIR spectrum. Many C—H alkene bending peaks can be observed in the range of 675–1000 cm^{-1} in BC, CBC and NBC (Nanda et al., 2013).

3.3. Conceivable adsorption mechanisms

Oxytetracycline determines a sensitivity for medium pH and under goes chemical speciation over a wide range of pH. Below 3.5 pH, OTC exists in cationic form while anionic form dominates beyond 7.5 pH. However, zwitterionic form of OTC is existed within the pH range of 3.5–7.5. Hydrolyzed urine reports a pH of 9 where OTC governs the anionic form (Premarathna et al., 2019). The best fitted model for BC demonstrates a physisorption mechanism. Negatively charged OTC molecules have the possibility to form weak bonds allowing multilayer adsorption, which is a layer by layer formation. Other than the weak Van der Waals forces, hydrogen bonding and dipolar attractions, pore-filling and film diffusion prominently governs physisorption (Ramanayaka et al., 2020a). Morphological features observed from SEM confirms the physisorption of OTC to CBC and NBC. Furthermore, it is clear that both hybrid sorption processes, including physisorption and chemisorption, are governed OTC adsorption on to CBC. Strong electrostatic bonding and covalent bonding exist in chemisorption, which is a monolayer formation process (Ahmed et al., 2015). However, both mechanisms can take place either at the same time or separately, which is not possible to be explained in the case of CBC. Moreover, NBC exhibited an interesting behavior in adsorption (Fig. 8). The isotherm graph demonstrates a two-step process, where the first step is governed by the Langmuir model while the second is Hills. Since it is two separate steps, one after one, we can conclude that monolayer forms by strong bonding and on top of the monolayer, multilayers be formed by weak bonds in between OTC molecules. However, the dominant adsorption mechanisms varied with many parameters such as medium pH, point of zero charges of the adsorbent material, speciation of adsorbate etc.

4. Conclusion

The adsorption of OTC onto BC, CBC, and NBC was investigated in synthetic hydrolyzed urine matrix. The highest adsorption capacity was obtained for CBC (136.7 mg/g). The adsorption of OTC onto biochar was successful and with respect to PC values, all three

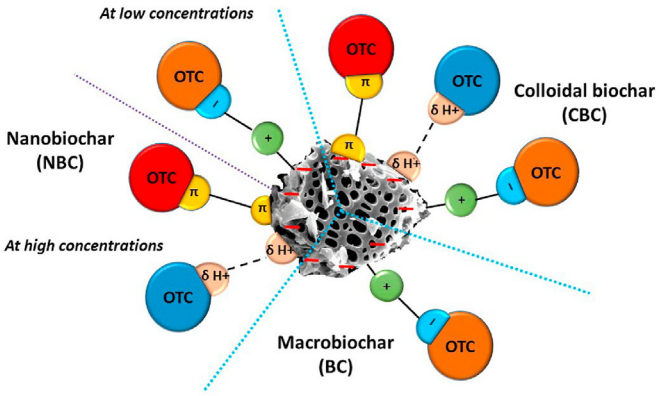

Fig. 8. Schematic diagram of possible adsorption mechanisms of oxytetracycline, to the charged surface of biochar through physisorption and chemisorption.

types of biochars behave with a similar performance in adsorbing OTC. During kinetic studies, BC and CBC were demonstrated chemisorption phenomena, while NBC exhibited both chemisorption and physisorption. Adsorption on to BC was governed by physisorption, while CBC depicted the involvement of hybrid processes. The Desorption of OTC back to urine is extremely low and BC, CBC, and NBC depicted a strong retention capacity. The obtained results widen the scope of biochar use for wastewater treatment, demonstrating CBC as a promising adsorbent for treating hydrolyzed human urine before application in agriculture or discharged into the environment. Nevertheless, limited desorption cycles, single adsorbent dosage and low yield of NBC are considered as limitations of this study. Removal of antibiotics from human urine using BC, CBC, and NBC can be further improved with simultaneous removal of a mixture of antibiotics which is possible to present in human urine. Furthermore, this study can be elaborate to assess the capacity of biochars from different feedstock materials, temperatures and also for modified biochars. The obtained results are possible to upgrade by conducting the same set of experiments with actual hydrolyzed human urine to confirm the applicability of BC, CBC, and NBC in future studies.

Credit author statement

Sammani Ramanayaka: Data curation, Formal analysis, writing original draft. Manish Kumar: writing-reviewing and editing. Thusitha Etampawala: Formal analysis, writing original draft. Meththika Vithanage: Conceptualization, funding acquisition, writing-reviewing and editing.

Declaration of competing interest

The authors declare that they have no known competing financial interests or personal relationships that could have appeared to influence the work reported in this paper.

Acknowledgments

We would like to acknowledge, Instrument Centre, Faculty of Applied Sciences, the University of Sri Jayewardenepura, Sri Lanka for instrument support. Surface area and pore analyses of this research were supported by the "Nanocomposites Research Group" at Faculty of Applied Sciences, the University of Sri Jayewardenepura set up by the Accelerating Higher Education Expansion and Development (AHEAD) Operation of the Ministry of Higher Education funded by the World Bank.

Appendix A. Supplementary data

Supplementary data to this article can be found online at https://doi.org/10.1016/j.envpol.2020.115683.

References

Aghababaei, A., Ncibi, M.C., Sillanpää, M., 2017. Optimized removal of oxytetracycline and cadmium from contaminated waters using chemically-activated and pyrolyzed biochars from forest and wood-processing residues. Bioresour. Technol. 239, 28–36. https://doi.org/10.1016/j.biortech.2017.04.119.

Ahadi, N., Sharifi, Z., Hossaini, S.M.T., Rostami, A., Renella, G., 2020. Remediation of heavy metals and enhancement of fertilizing potential of a sewage sludge by the synergistic interaction of woodlice and earthworms. J. Hazard. Mater. 385, 121573. https://doi.org/10.1016/j.jhazmat.2019.121573.

Ahmad, M., Rajapaksha, A.U., Lim, J.E., Zhang, M., Bolan, N., Mohan, D., Vithanage, M., Lee, S.S., Ok, Y.S., 2014. Biochar as a sorbent for contaminant management in soil and water: a review. Chemosphere 99, 19–33. https://doi.org/10.1016/j.chemosphere.2013.10.071.

Ahmed, M.B., Zhou, J.L., Ngo, H.H., Guo, W., 2015. Adsorptive removal of antibiotics from water and wastewater: progress and challenges. Sci. Total Environ. 532, 112–126. https://doi.org/10.1016/j.scitotenv.2015.05.130.

Arias, M.A., Arnold, U., Goldbach, H., 2019. Change in estrogenic activity in stored human urine before reuse as fertilizer. Int. J. Recycl. Org. Waste Agric. 8, 195–202. https://doi.org/10.1007/s40093-019-0289-z.

Ashiq, A., Sarkar, B., Adassooriya, N., Walpita, J., Rajapaksha, A.U., Ok, Y.S., Vithanage, M., 2019. Sorption process of municipal solid waste biochar-montmorillonite composite for ciprofloxacin removal in aqueous media. Chemosphere 236, 124384. https://doi.org/10.1016/j.chemosphere.2019.124384.

Ayawei, N., Ebelegi, A.N., Wankasi, D., 2017. Modelling and interpretation of adsorption isotherms. J. Chem. 1–11. https://doi.org/10.1155/2017/3039817.

Bandara, T., Herath, I., Kumarathilaka, P., Hseu, Z.-Y., Ok, Y.S., Vithanage, M., 2017. Efficacy of woody biomass and biochar for alleviating heavy metal bioavailability in serpentine soil. Environ. Geochem. Health 39, 391–401. https://doi.org/10.1007/s10653-016-9842-0.

Bischel, H.N., Duygan, B.D.Ö., Strande, L., McArdell, C.S., Udert, K.M., Kohn, T., 2015. Pathogens and pharmaceuticals in source-separated urine in eThekwini, South Africa. Water Res. 85, 57–65. https://doi.org/10.1016/j.watres.2015.08.022.

Farouq, R., Yousef, N.S., 2015. Equilibrium and kinetics studies of adsorption of copper (II) ions on natural biosorbent. Int. J. Chem. Eng. Appl. 6, 319. https://doi.org/10.7763/IJCEA.2015.V6.503.

Feng, L., Yuan, G., Xiao, L., Wei, J., Bi, D., 2020. Biochar modified by nano-manganese dioxide as adsorbent and oxidant for oxytetracycline. Bull. Environ. Contam. Toxicol. https://doi.org/10.1007/s00128-020-02813-0.

Foong, S.Y., Liew, R.K., Yang, Y., Cheng, Y.W., Yek, P.N.Y., Mahari, W.A.W., Lee, X.Y., Han, C.S., Vo, D.-V.N., Van Le, Q., 2020. Valorization of biomass waste to engineered activated biochar by microwave pyrolysis: progress, challenges, and future directions. Chem. Eng. J. 389, 124401. https://doi.org/10.1016/j.cej.2020.124401.

Fu, B., Ge, C., Yue, L., Luo, J., Feng, D., Deng, H., Yu, H., 2016. Characterization of biochar derived from pineapple peel waste and its application for sorption of oxytetracycline from aqueous solution. BioResources 11, 9017–9035. https://doi.org/10.15376/biores.11.4.9017-9035.

Garcıa, G., Faz, A., Cunha, M., 2004. Performance of Piptatherum miliaceum (Smilo grass) in edaphic Pb and Zn phytoremediation over a short growth period. Int. Biodeterior. Biodegrad. 54, 245–250. https://doi.org/10.1016/j.ibiod.2004.06.004.

Harja, M., Ciobanu, G., 2018. Studies on adsorption of oxytetracycline from aqueous solutions onto hydroxyapatite. Sci. Total Environ. 628, 36–43. https://doi.org/10.1016/j.scitotenv.2018.02.027.

Herath, I., Kumarathilaka, P., Navaratne, A., Rajakaruna, N., Vithanage, M., 2015. Immobilization and phytotoxicity reduction of heavy metals in serpentine soil using biochar. J. Soils Sediments 15, 126–138. https://doi.org/10.1007/s11368-014-0967-4.

Ji, K., Choi, Kyungho, Lee, S., Park, S., Khim, J.S., Jo, E.-H., Choi, Kyunghee, Zhang, X., Giesy, J.P., 2010. Effects of sulfathiazole, oxytetracycline and chlortetracycline on steroidogenesis in the human adrenocarcinoma (H295R) cell line and freshwater fish Oryzias latipes. J. Hazard. Mater. 182, 494–502. https://doi.org/10.1016/j.jhazmat.2010.06.059.

Ji, K., Kim, S., Han, S., Seo, J., Lee, S., Park, Y., Choi, Kyunghee, Kho, Y.-L., Kim, P.-G., Park, J., Choi, Kyungho, 2012. Risk assessment of chlortetracycline, oxytetracycline, sulfamethazine, sulfathiazole, and erythromycin in aquatic environment: are the current environmental concentrations safe? Ecotoxicology 21, 2031–2050. https://doi.org/10.1007/s10646-012-0956-6.

Jia, M., Wang, F., Bian, Y., Jin, X., Song, Y., Kengara, F.O., Xu, R., Jiang, X., 2013. Effects of pH and metal ions on oxytetracycline sorption to maize-straw-derived biochar. Bioresour. Technol. 136, 87–93. https://doi.org/10.1016/j.biortech.2013.02.098.

Katsikaros, A.G., Chrysikopoulos, C.V., 2020. Estimation of urine volume in municipal sewage originating from patients receiving antibiotics at a private clinic in Crete, Greece. Sci. Total Environ. 705, 134858. https://doi.org/10.1016/j.scitotenv.2019.134858.

Kaufmann, A., Butcher, P., Maden, K., Widmer, M., 2007. Ultra-performance liquid chromatography coupled to time of flight mass spectrometry (UPLC–TOF): a novel tool for multiresidue screening of veterinary drugs in urine. Anal. Chim. Acta 586, 13–21. https://doi.org/10.1016/j.aca.2006.10.026.

Kong, S., Lam, S.S., Yek, P.N.Y., Liew, R.K., Ma, N.L., Osman, M.S., Wong, C.C., 2019. Self-purging microwave pyrolysis: an innovative approach to convert oil palm shell into carbon-rich biochar for methylene blue adsorptionKong S, Lam SS, Yek PNY, et al (2019) Self-purging microwave pyrolysis: an innovative approach to convert oil palm she. J. Chem. Technol. Biotechnol. 94, 1397–1405. https://doi.org/10.1002/jctb.5884.

Kong, W., Li, C., Dolhi, J.M., Li, S., He, J., Qiao, M., 2012. Characteristics of oxytetracycline sorption and potential bioavailability in soils with various physical–chemical properties. Chemosphere 87, 542–548. https://doi.org/10.1016/j.chemosphere.2011.12.062.

Li, Z., Sun, Y., Yang, Y., Han, Y., Wang, T., Chen, J., Tsang, D.C.W., 2020. Comparing biochar-and bentonite-supported Fe-based catalysts for selective degradation of antibiotics: mechanisms and pathway. Environ. Res. 183, 109156. https://doi.org/10.1016/j.envres.2020.109156.

Lin, Y.-B., Fugetsu, B., Terui, N., Tanaka, S., 2005. Removal of organic compounds by alginate gel beads with entrapped activated carbon. J. Hazard. Mater. 120, 237–241. https://doi.org/10.1016/j.jhazmat.2005.01.010.

Luo, J., Li, X., Ge, C., Müller, K., Yu, H., Huang, P., Li, J., Tsang, D.C.W., Bolan, N.S., Rinklebe, J., Wang, H., 2018. Sorption of norfloxacin, sulfamerazine and oxytetracycline by KOH-modified biochar under single and ternary systems. Bioresour. Technol. 263, 385–392. https://doi.org/10.1016/j.biortech.2018.05.022.

Maillard, É., Angers, D.A., 2014. Animal manure application and soil organic carbon stocks: a meta-analysis. Global Change Biol. 20, 666–679. https://doi.org/10.1111/gcb.12438.

Manna, S., Singh, N., Purakayastha, T.J., Berns, A.E., 2020. Effect of deashing on physico-chemical properties of wheat and rice straw biochars and potential sorption of pyrazosulfuron-ethyl. Arab. J. Chem. 13, 1247–1258. https://doi.org/10.1016/j.arabjc.2017.10.005.

Mayakaduwa, S.S., Kumarathilaka, P., Herath, I., Ahmad, M., Al-Wabel, M., Ok, Y.S., Usman, A., Abduljabbar, A., Vithanage, M., 2016. Equilibrium and kinetic mechanisms of woody biochar on aqueous glyphosate removal. Chemosphere 144, 2516–2521. https://doi.org/10.1016/j.chemosphere.2015.07.080.

Medeiros, D.L., Queiroz, L.M., Cohim, E., Almeida-Neto, J.A. de, Kiperstok, A., 2020. Human urine fertiliser in the Brazilian semi-arid: environmental assessment and water-energy-nutrient nexus. Sci. Total Environ. 713, 136145. https://doi.org/10.1016/j.scitotenv.2019.136145.

Nafi, E., Webber, H., Danso, I., Naab, J.B., Frei, M., Gaiser, T., 2020. Interactive effects of conservation tillage, residue management, and nitrogen fertilizer application on soil properties under maize-cotton rotation system on highly weathered soils of West Africa. Soil Tillage Res. 196, 104473. https://doi.org/10.1016/j.still.2019.104473.

Nanda, S., Mohanty, P., Pant, K.K., Naik, S., Kozinski, J.A., Dalai, A.K., 2013. Characterization of North American lignocellulosic biomass and biochars in terms of their candidacy for alternate renewable fuels. BioEnergy Res. 6, 663–677. https://doi.org/10.1007/s12155-012-9281-4.

Ogunfowokan, A.O., Adekunle, A.S., Oyebode, B.A., Oyekunle, J.A.O., Komolafe, A.O., Omoniyi-Esan, G.O., 2019. Determination of heavy metals in urine of patients and tissue of corpses by atomic absorption spectroscopy. Chem. Africa 2, 699–712. https://doi.org/10.1007/s42250-019-00073-y.

Pandorf, M., Hochmuth, G., Boyer, T.H., 2018. Human urine as a fertilizer in the cultivation of snap beans (Phaseolus vulgaris) and turnips (Brassica rapa). J. Agric. Food Chem. 67, 50–62. https://doi.org/10.1021/acs.jafc.8b06011.

Park, S., Choi, K., 2008. Hazard assessment of commonly used agricultural antibiotics on aquatic ecosystems. Ecotoxicology 17, 526–538. https://doi.org/10.1007/s10646-008-0209-x.

Pradhan, S.K., Nerg, A.-M., Sjöblom, A., Holopainen, J.K., Heinonen-Tanski, H., 2007. Use of human urine fertilizer in cultivation of cabbage (Brassica oleracea)––impacts on chemical, microbial, and flavor quality. J. Agric. Food Chem. 55,

8657–8663. https://doi.org/10.1021/jf0717891.
Premarathna, K.S.D., Rajapaksha, A.U., Adassoriya, N., Sarkar, B., Sirimuthu, N.M.S., Cooray, A., Ok, Y.S., Vithanage, M., 2019. Clay-biochar composites for sorptive removal of tetracycline antibiotic in aqueous media. J. Environ. Manag. 238, 315–322. https://doi.org/10.1016/j.jenvman.2019.02.069.
Qian, L., Zhang, W., Yan, J., Han, L., Gao, W., Liu, R., Chen, M., 2016. Effective removal of heavy metal by biochar colloids under different pyrolysis temperatures. Bioresour. Technol. 206, 217–224. https://doi.org/10.1016/j.biortech.2016.01.065.
Ramanayaka, S., Sarkar, B., Cooray, A.T., Ok, Y.S., Vithanage, M., 2020a. Halloysite nanoclay supported adsorptive removal of oxytetracycline antibiotic from aqueous media. J. Hazard. Mater. 384 https://doi.org/10.1016/j.jhazmat.2019.121301.
Ramanayaka, S., Tsang, D.C.W., Hou, D., Ok, Y.S., Vithanage, M., 2020b. Green synthesis of graphitic nanobiochar for the removal of emerging contaminants in aqueous media. Sci. Total Environ. 706 https://doi.org/10.1016/j.scitotenv.2019.135725.
Rao, M.M., Ramana, D.K., Seshaiah, K., Wang, M.C., Chien, S.W.C., 2009. Removal of some metal ions by activated carbon prepared from Phaseolus aureus hulls. J. Hazard. Mater. 166, 1006–1013. https://doi.org/10.1016/j.jhazmat.2008.12.002.
Saadi, R., Saadi, Z., Fazaeli, R., Fard, N.E., 2015. Monolayer and multilayer adsorption isotherm models for sorption from aqueous media. Kor. J. Chem. Eng. 32, 787–799. https://doi.org/10.1007/s11814-015-0053-7.
Segun Esan, O., Nurudeen Abiola, O., Owoyomi, O., Olumuyiwa Aboluwoye, C., Olubunmi Osundiya, M., 2014. Adsorption of brilliant green onto luffa cylindrical sponge: equilibrium, kinetics, and thermodynamic studies. ISRN Phys. Chem. https://doi.org/10.1155/2014/743532.
Sivagami, K., Vignesh, V.J., Srinivasan, R., Divyapriya, G., Nambi, I.M., 2020. Antibiotic usage, residues and resistance genes from food animals to human and environment: an Indian scenario. J. Environ. Chem. Eng. 8, 102221. https://doi.org/10.1016/j.jece.2018.02.029.
Solanki, A., Boyer, T.H., 2017. Pharmaceutical removal in synthetic human urine using biochar. Environ. Sci. Water Res. Technol. 3, 553–565. https://doi.org/10.1039/C6EW00224B.
Sun, P., Li, Y., Meng, T., Zhang, R., Song, M., Ren, J., 2018. Removal of sulfonamide antibiotics and human metabolite by biochar and biochar/H2O2 in synthetic urine. Water Res. 147, 91–100. https://doi.org/10.1016/j.watres.2018.09.051.
Tian, H., Jiao, J., Yu, X., Zha, F., Tang, X., Guo, X., Chang, Y., 2020. Synergic adsorption performance of activated carbon prepared from Chinese prickly ash seeds. Environ. Technol. 1–16. https://doi.org/10.1080/09593330.2020.1797892.
Tong, X., Li, J., Yuan, J., Xu, R., 2011. Adsorption of Cu(II) by biochars generated from three crop straws. Chem. Eng. J. 172, 828–834. https://doi.org/10.1016/j.cej.2011.06.069.
Vikrant, K., Kim, K.-H., 2019. Nanomaterials for the adsorptive treatment of Hg (II) ions from water. Chem. Eng. J. 358, 264–282. https://doi.org/10.1016/j.cej.2018.10.022.
Wang, Z., Yang, X., Qin, T., Liang, G., Li, Y., Xie, X., 2019. Efficient removal of oxytetracycline from aqueous solution by a novel magnetic clay–biochar composite using natural attapulgite and cauliflower leaves. Environ. Sci. Pollut. Res. 26, 7463–7475. https://doi.org/10.1007/s11356-019-04172-8.
Wijesekara, S.S.R.M.D.H.R, Mayakaduwa, S.S., Siriwardana, A.R., de Silva, N., Basnayake, B.F.A., Kawamoto, K., Vithanage, M., 2014. Fate and transport of pollutants through a municipal solid waste landfill leachate in Sri Lanka. Environ. Earth Sci. 72, 1707–1719. https://doi.org/10.1007/s12665-014-3075-2.
Wu, F.-C., Tseng, R.-L., Juang, R.-S., 2009. Characteristics of Elovich equation used for the analysis of adsorption kinetics in dye-chitosan systems. Chem. Eng. J. 150, 366–373. https://doi.org/10.1016/j.cej.2009.01.014.
Xu, K., Lin, F., Dou, X., Zheng, M., Tan, W., Wang, C., 2018. Recovery of ammonium and phosphate from urine as value-added fertilizer using wood waste biochar loaded with magnesium oxides. J. Clean. Prod. 187, 205–214. https://doi.org/10.1016/j.jclepro.2018.03.206.
Yang, W., Yu, Z., Pan, B., Lv, L., Zhang, W., 2015. Simultaneous organic/inorganic removal from water using a new nanocomposite adsorbent: a case study of p-nitrophenol and phosphate. Chem. Eng. J. 268, 399–407. https://doi.org/10.1016/j.cej.2015.01.051.
Zhang, R., Sun, P., Boyer, T.H., Zhao, L., Huang, C.-H., 2015. Degradation of pharmaceuticals and metabolite in synthetic human urine by UV, UV/H2O2, and UV/PDS. Environ. Sci. Technol. 49, 3056–3066. https://doi.org/10.1021/es504799n.